

Localization concepts applied to the analysis of reinforced concrete deep beams

T.Lertsrisakulrat, T.Miki, M.Matsuo & J.Niwa
Tokyo Institute of Technology, Tokyo, Japan

ABSTRACT: A bending test program on the series of RC deep beams with the effective depth, d , of 200, 400 and 600 mm has been performed. The transverse reinforcement ratio was varied from 0.0, 0.4 to 0.8 percent. The distribution of the local strains inside specimens, both of concrete and reinforcement, has been measured. The test results confirm the localized compressive failure of concrete in the deep beams. Subsequently, the localized failure volume, V_p , and the fracture energy, G_{Fc} , of the concrete which locally failed in compression of each beam specimen have been evaluated. Finally, the concepts of localized compressive failure of concrete have been incorporated in the analysis of deep beam using Lattice model and the comparison between the experimental and analytical results has been done.

1 INTRODUCTION

The behavior of reinforced concrete beams at failure in shear is distinctly different from their behavior in flexure as the failure occurs abruptly without sufficiently advanced warning. Furthermore, the diagonal cracks that develop are considerably wider than the flexural cracks, especially, for deep beams in which shear is being the significant parameter. Deep beams are structural elements having a shear span to effective depth ratio, a/d , not exceeding 1. Due to the geometry of deep beams, they behave as two-dimensional rather than one-dimensional members and are subjected to a two-dimensional state of stress. As a result, plane sections before bending do not necessarily remain plane after bending. The resulting strain distribution can be no longer considered as linear, and shear deformations that are neglected in normal beams become significant compared to pure flexure. Consequently, the stress distribution acting on the cross-section of the beam becomes nonlinear even at the elastic stage. At the ultimate limit state, the compressive stress distribution in the concrete would no longer be the same parabolic shape as in the normal beam.

At the final failure state of deep beams, the upper portion of the beams in the vicinity area under the location in which the load is applied, the crushing of concrete due to compression is usually observed, together with the compressive failure along the compressive arch directions (diagonal cracks) which

connecting between the loading point and supports. Owing to the fact that the failure of concrete in compression is localized (Santiago & Hilsdorf 1973, Lertsrisakulrat et al., in press, Markeset 1993), the descending path of the stress-strain curve is size-dependent and cannot be considered as material property. For this reason, in the analysis of reinforced concrete beams, more accurate results can be expected if the effects of localization in compression are taken into account.

Therefore, in this paper, an experimental program on a series of deep beams with and without transverse reinforcement subjected to the concentrated load at the mid span has been conducted in order to observe the actual compressive shear failure behavior. By utilizing the techniques of local strain measurement (Nakamura & Higai 1999), the observation on the localized compressive failure of the RC deep beams has been carried out. Subsequently, the localized compressive failure volume has been evaluated and the fracture energy of the concrete which failed in compression in the deep beams has been evaluated. Finally, the comparison between the experimental and the analytical results has been done.

2 EXPERIMENTS FOR OF DEEP BEAMS

2.1 *Outlines of the experiments*

Deep beams with the effective depth, d , of 200, 400 and 600 mm and the loading span, $2a$, of 400, 800

Table 2. Mixing proportion and mechanical properties of reinforcements.

(a) Mixing proportion.						(b) Mechanical properties of reinforcements.					
W/C	s/a	Unit content (kg/m ³)				Reinforcement	Size/Grade	Area	E _s	f _y	f _u
%	%	W	C	S	G		mm ²	N/mm ²	N/mm ²	N/mm ²	
50	49	190	380	853	898	Top Bar	R6/SR235	28.27	-	310	452
C:high early strength portland cement; S:river sand; G:crushed stone, max. size=13mm; age of test 7 days (excepts D404, 49 days); air content 2.5%; no water reducing agent or superplasticizer.						Vertical Steel	D6/SD295A	31.67	-	331	509
						Deformed	PC-φ 19	286.50	2.01 × 10 ⁵	1026	1127
						PC Bar	PC-φ 25	506.70	2.00 × 10 ⁵	1004	1130
						(Type B)	PC-φ 32	794.20	2.01 × 10 ⁵	1006	1147

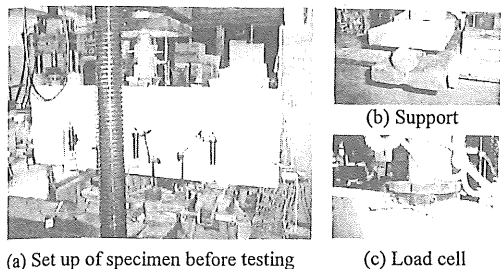


Figure 4. Test set up.

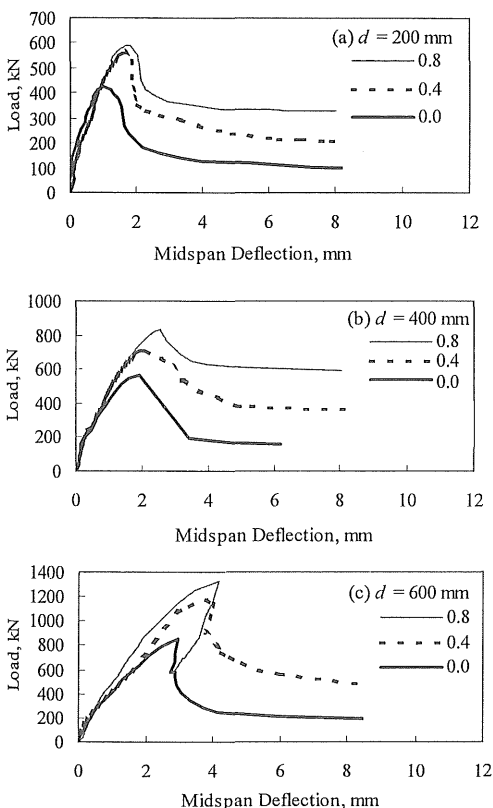


Figure 5. Load-mid span deflection curves of the tested beams. also attached to the reinforcements. Figures 3a, b show the photos of the beams before casting and the local strain gages embedded inside the specimen.

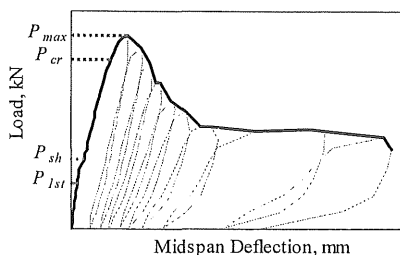


Figure 6. Typical test results.

The concrete mixed with the maximum aggregate size 13 mm was used in casting of the beams. The mixing proportion and the mechanical properties of the reinforcements are summarized in Table 2a, b.

All beams were subjected to the concentrated load at the mid span through the loading plate, width r , as shown in Table 1 ($r/d=0.25$). At each support, a set of teflon sheets inserted by silicon grease was put over the steel plate (which has the same width as the loading plate, r), in order to reduce the friction at the interface between the specimen and the supports and to ensure the horizontal movement of the specimen during the test. The deflection of the beam was measured by using deflection gages measured at both faces of the mid span and over the both supports. The horizontal movement of the beams has also been checked by a deflection gages installed horizontally at either end of a specimen. The test set up and the measurement were illustrated as shown in Figure 4. During all tests, the occurrence and the propagation of cracks have been visually detected. After the peak load was reached, the technique of one-directional repeated loading was utilized in order to capture the complete load-deflection curve.

2.2 Experimental results

From the test results, the load-mid span deflection curve of the beams can be plotted as shown in Figures 5a-c, whereas Figure 6 shows the typical load-mid span deflection curve. All test results are tabulated in Table 3.

On the other hand, from the local strains meas-

Table 3. Test results.

Specimen	P_{jst} kN	P_{shr} kN	P_{cr} kN	P_{max} kN	f_c' N/mm ²	f_l N/mm ²	$V_p \times 10^6$ mm ³	E_{net} kN-mm	G_{Fc} N/mm ²	G_{Fc}^{***} N/mm ²
D200	125.6	157.0	304.1	428.3	38.4	3.4	3.50	802	0.229	0.214
D204	107.9	215.8	-	559.5	43.2	2.7	3.50	1064	0.304	0.220
D208	104.0	145.2	578.8	591.4	34.2	3.1	3.50	1313	0.375	0.208
D400	127.5	181.5	155.0	570.6	35.5	3.0	6.30	1420	0.225	0.210
D404	137.3	235.4	627.8	711.8	27.5	2.8	11.20	2231	0.199	0.197
D408	196.2	274.7	735.8	827.9	38.4	3.4	9.80	2173	0.222	0.214
D600	215.8	245.3	588.6	848.9	40.8	2.4	16.80	2671	0.159	0.217
D604	206.0	284.5	-	1173.3	34.2	3.1	19.95	3861	0.194	0.208
D608	299.2	377.7	1314.5	1327.6	35.3	3.1	23.10	5591***	0.242	0.210

*Results not available ** G_{Fc} is the compressive fracture energy of concrete when subjected to uniaxial compressive force.

*** E_{net} of D608 was estimated from the internal measurement

**** The fracture energy of concrete in tension, G_F is 0.16 N/mm for all cases.

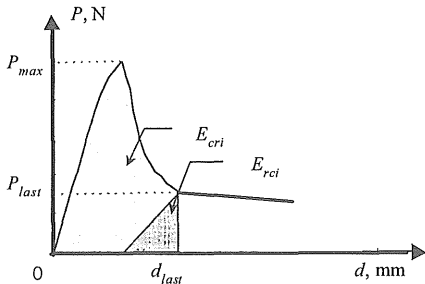


Figure 7. Calculation of E_{cri} .

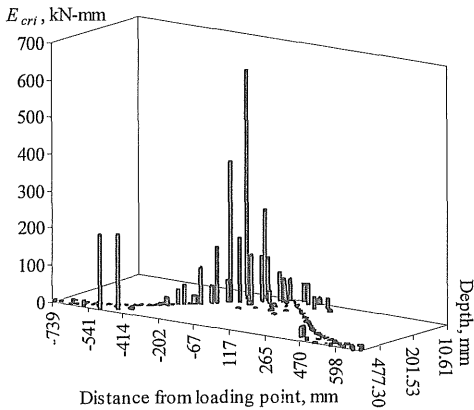


Figure 8. Distribution of E_{cri} .

urement, the local displacement can be obtained by multiplying the measured local strain by the interval between each strain gage, i.e. 30 or 60 mm, then the relative energy consumed locally by concrete, E_{cri} , can be calculated from the area under the load-local displacement curve of each gage excluding the recoverable portion, E_{rci} (Fig. 7). The sample of the distribution of E_{cri} plotted in Figure 8 shows that only some portions of concrete absorbed most of the energy while some portions absorbed very small or almost zero amount of energy. That means, when a

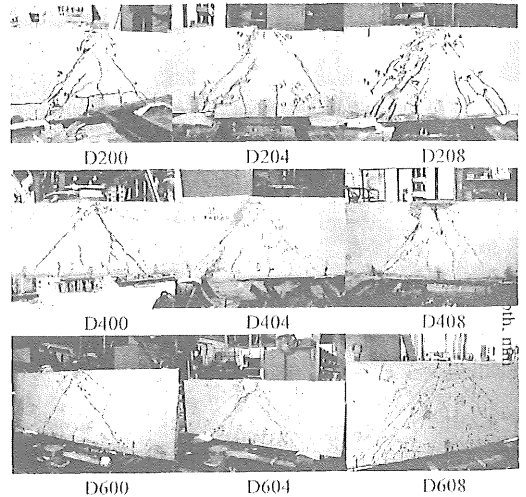


Figure 9. Failure of the specimens.

deep beam failed in compressive shear, the localization in compression occurred along the compressive arch directions, which connecting between the point of load application and supports, and in vicinity of the loading point. The determination of the compressive localized failure volume of the concrete in deep beams will be discussed later in section 3.1

In the test, the compressive failure mode and adequate concrete covering of the beam were enhanced by employing the high strength deformed PC bars. In addition, according to the results from the strain gages attached to the PC bars at the mid span, it was found that the maximum stress of the bars are far below the yielding limit in all cases.

2.3 Failure of deep beams

Cracking started with the development of a few fine vertical flexural cracks at the mid span, at the first cracking load, P_{jst} . Then, few inclined shear cracks suddenly developed and proceeded to propagate to-

ward the neutral axis from the supports to the portion in which the external load was applied as it can be seen from the swiftly change of the slope of the load-deformation curve when the shear cracking load, P_{sh} , was reached (Fig.6). When the beam was further loaded, the crushing of concrete in the vicinity of the loading point began at the crushing load, P_{cr} . Finally, the beam reached the maximum resistance at the peak load, P_{max} , and the failure took place as the principal inclined crack dynamically joined the crushed concrete zone.

However, it was observed that the severe failure generally took place only at one side of the beam. This is because of the fact that a reinforced concrete beam is not homogeneous and the strength of the concrete throughout the span is subjected to a normally distributed variation, hence the stabilized failure of diagonal cracks at both ends of the beam cannot be expected as can be seen from the photos shown in Figure 9.

3 PARAMETERS OF THE LOCALIZED COMPRESSIVE FAILURE

3.1 Localized compressive failure volume, V_p

According to Figure 8, the compressive localized failure zone can then be quantitatively judged based on the calculated E_{cri} . From the external load-local strain distribution relationship along the compressive arch directions, it was found that the failure always concentrated on one side, while another side showed unloading behavior. Therefore, the failure portion is judged by the portion in which E_{cri} is larger than 3 percent of the summation of E_{cri} of all gages along the direction of the failure side of the compressive arch (acrylic bar a or b, Figures 2a-c), E_{cr} . The criterion of 3 percent has been selected based on the comparison with the photos taken after the tests, in accordance with the consideration on the shape of the external load-local strain distribution curves. Then, the localized compressive failure length, L_p , of concrete can be determined and V_p is the result of L_p multiplies by the width of the compressive arch, w_p ,

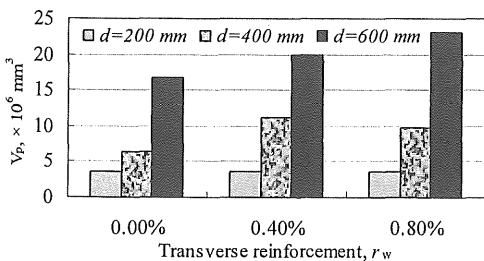


Figure 10. Localized compressive failure volume, V_p .

and the width of the beam (150 mm). Here, the width of compressive arch is calculated from the summation of the width of the bearing plate, r , and the 0.3 times the effective depth of the beam divided by $\sin 45$, as shown in Equation 1. The value of w_p was taken from the previous research of Niwa (1984).

$$w_p = (r + 0.3d) / \sin 45 \quad (1)$$

The results of V_p are summarized in Table 3. It is noted that, for D608, the failure pattern of the beam was different from the other cases. The failure of fan-like shape was observed; therefore, V_p is obtained from the actual failure volume measured by the local strain gages embedded inside.

Figure 10 shows the value of V_p obtained from the experiment. The tendency of, somehow, increasing in V_p was observed when the transverse reinforcement was increased. However, in case of $d = 200$ mm, the constant value of V_p was observed (in other words, the failure occurred throughout the compressive arch in all cases). That means the localization in compression did not occur when $d = 200$ mm.

3.2 Compressive fracture energy, G_{Fc}

Subsequently, the fracture energy of concrete, which failed in compression, G_{Fc} , is computed based on the obtained V_p and the externally applied energy that caused localized compressive failure to concrete, E_{net} . Because G_{Fc} is defined as the energy required to cause compressive failure to a unit volume of concrete, thus the effects of the reinforcements such as confinement from the stirrups, and the effects of the friction between the loading plate and the specimen, which consumed some parts of externally applied energy, should be taken into account properly.

For the beams without transverse reinforcement, at the first step, E_{ext} is calculated from the area under load-mid span deflection curve excluding the part that can be recovered when unloaded, E_{rc} (the same concept as E_{cri} and E_{rci} , Fig. 7). Then, E_{net} is obtained by multiplying E_{ext} by the localized factor, K_l , which is the ratio of the summation of the relative energy, E_{cri} , consumed by the failure portion to the total relative energy consumed along the compressive arch directions. The factor K_l has been introduced in order that the fraction of the externally applied energy which was consumed by the friction force (or also from the effects of the confinement from the stirrups in case of specimen with transverse reinforcement) will be taken into account. It was found that the value of K_l is ranging from 80-90%.

For beams with transverse reinforcement, the en-

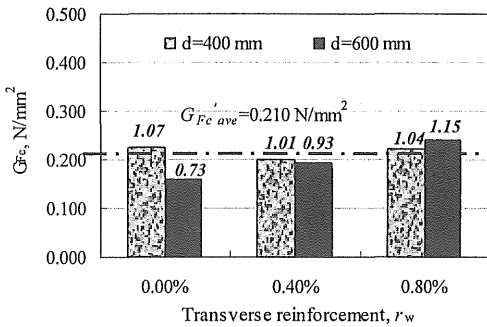


Figure 11. Compressive fracture energy, G_{F_c} .

ergy consumed by the yielded reinforcements, E_{yield} , calculated from the measured local strain of the reinforcements, i.e. top bars or transverse reinforcements, must be excluded from the E_{ext} before multiplying by K_1 as shown in Equation 2.

$$E_{net} = K_1 (E_{ext} - E_{yield}) \quad (2)$$

Then, G_{F_c} is obtained by dividing the E_{net} by V_p , as shown in Equation 3 and the results have been summarized in Table 3.

$$G_{F_c} = E_{net} / V_p \quad (\text{N/mm}^2) \quad (3)$$

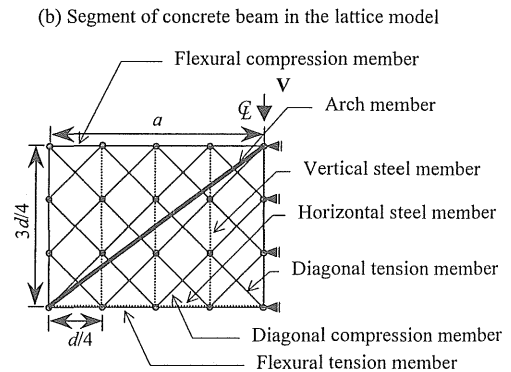
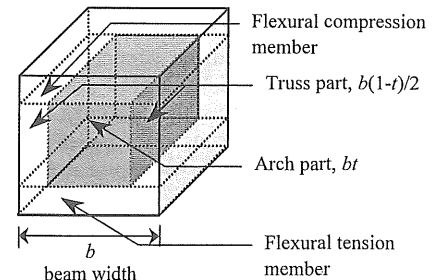
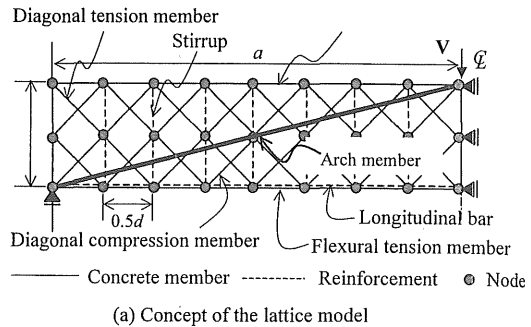
It should be noted that the calculation of energy was done up to the point in which the gradient of the descending path of the curve became flat, that is when the mid span deflection, d_{last} , equal to 4, 6 and 10 mm for the case of $d = 200, 400$ and 600 mm, respectively.

Furthermore, according to authors' previous research (Lertsrisakulrat et al., in press), it has been found that the relationship between the concrete cylindrical compressive strength, f'_c , and the concrete compressive fracture energy when subjected to uniaxial compressive load, G_{F_c} , can be shown by the following Equation 4.

$$G_{F_c}' = 0.86 \times 10^{-1} f'_c{}^{1/4} \quad (\text{N/mm}^2) \quad (4)$$

Then, the comparison between G_{F_c} , obtained from the deep beam tests, and G_{F_c}' , from the uniaxial compressive tests, has been proceeded. The results are plotted as shown in Figure 11. The numbers shown in the curve are the value of G_{F_c} compare with G_{F_c}' , i.e. G_{F_c} / G_{F_c}' . Noted that the results of the $d=200$ series were not included here because the localized compressive failure of the beam was not taken place, and the E_{net} used in calculation of G_{F_c} in case of D608 was estimated from the summation of E_{cri} of all the strain gages attached to the deformed acrylic bars divided by the square root of 2.

It can be seen that the results of G_{F_c} from the deep beam tests agree very well with the results of the uniaxial compressive tests when the energy con-



(c) Aspects of lattice model in this analysis

Figure 12. Modeling of element in the lattice model.

sumed by concrete was properly evaluated. That means the concept of localization in compression can be applied to the reinforced concrete deep beams as well as in case of uniaxial compression. In other words, when a concrete member is subjected to the compressive load, the localized failure occurs and the failure volume is depended on the externally applied energy which consumed by the concrete, in such a way that the externally applied energy per unit failure volume, i.e. G_{F_c} , become constant.

4 LATTICE MODEL ANALYSIS

As mentioned above, the conventional beam theory is not applicable to the D-region where the strain

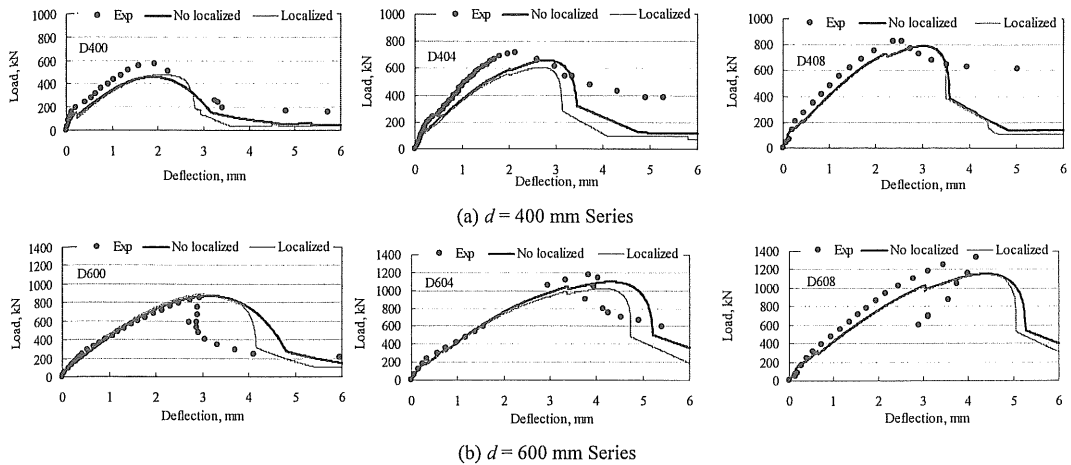


Figure 13. Comparison of the experimental and analytical results ($d = 400$ and 600 mm series).

distribution is significantly nonlinear. This is the case of this study, where deep beams are subjected to concentrated load at the mid span. Therefore, in the analysis, the lattice model (Niwa et al. 1995) which is a simple analytical model to clarify the change in the shear resisting mechanism before and after a diagonal cracking of reinforced concrete members, has been adopted. The continuum body of the reinforced concrete deep beam is converted into an assembly of truss components in which the arch member was introduced in order to take into account the influence of the internal compressive stress flow, as shown in Figure 12.

As it can be seen from the final failure pattern of the specimen that the localized compressive failure occurred along the direction of the arch element (the direction of diagonal cracks), hence in the analysis, using the lattice model, the effect of the localization in compression was incorporated into the arch elements.

Here, only the comparison between experimental and analytical results of $d = 400$ and 600 mm series will be carried out, because in case of $d = 200$ mm the localization in compression along the compressive arch member did not occur.

5 COMPARISONS BETWEEN THE EXPERIMENTAL AND ANALYTICAL RESULTS

Figure 13a, b show the comparison between the experimental and analytical results. The analytical results included the results before the effects of the localization in compression were taken into consideration. It can be seen that the prediction considering the effects of the localization in compression shows a, somehow, better prediction of the de-

scending path of the load-deflection curves. Nevertheless, in case of high transverse reinforcement ratio, i.e. $r_w = 0.8\%$, it was found that even the effects of the localization in compression were taken into account, the results were not much different from the case in which the localized compressive failure was not taken into considerations. That is because the compressive failure lengths, L_p , are almost the same as the length of the arch members in the model itself.

6 CONCLUSIONS

From the experimental results, by measuring the strain distributions inside RC deep beams, the occurrence of concrete localized compressive failure in the deep beams has been confirmed. The compressive localized failure volume can be determined based on the measured local strain and relative energy consumed by concrete. Subsequently, the compressive fracture energy of concrete has been determined based on the obtained compressive localized failure volume and the externally applied energy that caused the compressive failure of concrete. The results show very good agreement between the deep beam tests and the uniaxial compressive tests, when the energy was evaluated properly. Finally, the comparison between the obtained experimental results of the deep beams and the analytical results using the lattice model taking into account the localization failure in compression, in terms of the load-deflection curves has been conducted. It was found that the better prediction of the load-deformation curve was obtained when the effects of the localized failure in compression was taken in to account.

REFERENCES

- Lertsrisakulrat, T. et. al., in press. Experimental study on parameters in localization of concrete subjected to compression. *Journal of Materials, Concrete Structures and Pavements, JSCE*.
- Markeset, G. 1993. Failure of concrete under compressive strain gradients. *Dr.Eng thesis, Norwegian Institute of Technology, Trondheim*.
- Nakamura, H. & Higai, T. 1999. Compressive fracture energy and fracture zone length of concrete. *JCI-C51E Seminar on Post-Peak Behavior of RC Structures Subjected to Seismic Loads 2:259-272*.
- Niwa, J. 1984. Equation for shear strength of reinforced concrete deep beams based on FEM analysis. *Concrete Library of JSCE 4:283-295*.
- Niwa, J. et. al. 1995. Analytical Study for Shear Resisting Mechanism Using Lattice Model. *Concrete Library of JSCE 26:95-109*.
- Santiago, S.D. & Hilsdorf, H.K. 1973. Fracture mechanisms of concrete under compressive loads. *Cement and Concrete Research 3:363-388*.